β-decay Q values among the $A = 50$ Ti-V-Cr isobaric triplet and atomic masses of ^{46,47,49,50}Ti, ^{50,51}V, and $^{50,52–54}$Cr

R. M. E. B. Kandegedara,[1] G. Bollen,[2,3] M. Eibach,[4,5] N. D. Gamage,[1,6] K. Gulyuz,[4] C. Izzo,[3,4] M. Redshaw,[1,4,6,*] R. Ringle,[4] R. Sandler,[1,3,4,6] and A. A. Valverde[3,4,†]

[1]*Department of Physics, Central Michigan University, Mount Pleasant, Michigan 48859, USA*
[2]*Facility for Rare Isotope Beams, East Lansing, Michigan 48824, USA*
[3]*Department of Physics and Astronomy, Michigan State University, East Lansing, Michigan 48824, USA*
[4]*National Superconducting Cyclotron Laboratory, East Lansing, Michigan 48824 USA*
[5]*Universität Greifswald, 17487 Greifswald, Germany*
[6]*Science of Advanced Materials Program, Central Michigan University, Mount Pleasant, Michigan 48859, USA*

(Received 7 August 2017; published 20 October 2017)

Using high-precision Penning trap mass spectrometry at the Low Energy Beam and Ion Trap facility at the National Superconducting Cyclotron Laboratory we have measured the Q values of the fourth-order forbidden β decay and electron capture of ^{50}V and the double electron capture Q value of ^{50}Cr with the results $Q_\beta(^{50}\mathrm{V}) = 1038.1(1)$ keV, $Q_{\mathrm{EC}}(^{50}\mathrm{V}) = 2208.7(1)$ keV, and $Q_{2\mathrm{EC}}(^{50}\mathrm{Cr}) = 1170.5(1)$ keV. In addition, we have measured the atomic masses of ^{46,47,49,50}Ti, ^{50,51}V, and $^{50,52–54}$Cr, reducing uncertainties by factors of up to three compared with the most recent atomic mass evaluation (AME2016) [Chin. Phys. C **41**, 030003 (2017)]. Our results are in good agreement with AME2016 for ^{46,47,49,50}Ti and ^{50,54}Cr and show deviations of up to $\sim$1 keV (2.5σ) for ^{50,51}V and ^{50,54}Cr.

DOI: 10.1103/PhysRevC.96.044321

I. INTRODUCTION

In nature, only three nuclei are known to exist for which the dominant decay process is a fourfold forbidden nonunique β decay. ^{50}V stands alone among the three in that it can undergo electron capture (EC)—to the 2^+ state in ^{50}Ti—or β-decay—to the 2^+ state in ^{50}Cr (see the decay scheme in Fig. 1). The other two, ^{113}Cd and ^{115}In, both undergo β decay to the ground states of their respective daughter nuclides. The fact that ^{50}Cr is more strongly bound than ^{50}V but less so than ^{50}Ti means that ^{50}Cr is unstable against double electron capture (2EC) to the ^{50}Ti ground state. Experimental searches for all three decays in this isobaric triplet have been undertaken, e.g., most recently in Refs. [1,2].

The electron-capture decay of ^{50}V to ^{50}Ti(2^+) was first observed in 1984 by Alburger *et al.* [3] and in further experiments in the 1980s by Simpson *et al.* [4,5]. The half-life was measured recently and more precisely by using modern low-background techniques, with the result $T_{1/2}^{\mathrm{EC}} = (2.29 \pm 0.25) \times 10^{17}$ yr [1]. Attempts to observe ^{50}V β decay to ^{50}Cr(2^+) have produced only lower limits on the half-life for this decay branch, except for one claimed observation [5]. However, this result was not confirmed by the recent experiment of Ref. [1], which saw no indication of this decay branch and provided a lower limit $T_{1/2}^{\beta} > 1.5 \times 10^{18}$ yr. Recent theoretical descriptions of ^{50}V electron capture and β decay have provided calculated half-lives of $\approx 4 \times 10^{17}$ yr and $\approx 2 \times 10^{19}$ yr for the electron-capture and β-decay modes, respectively [6]. The calculated electron-capture half-life is in good agreement with the experimental observations, and the calculated β-decay half-life indicates that this decay could be observed in an experiment with existing low-background facilities and an achievable increase in source material.

In this paper, we report on the first direct determination of the Q values $Q_{\mathrm{EC}}(^{50}\mathrm{V} \rightarrow {}^{50}\mathrm{Ti})$, $Q_\beta(^{50}\mathrm{V} \rightarrow {}^{50}\mathrm{Cr})$, and $Q_{2\mathrm{EC}}(^{50}\mathrm{Cr} \rightarrow {}^{50}\mathrm{Ti})$ using high-precision Penning trap mass spectrometry. These data provide precise inputs for determinations of the phase space factors that appear in the theoretical descriptions of the decays to determine the partial half-lives. In the case of β decay the phase-space factor appears in the calculation of the spectral shape, which is of interest for comparing theoretical predictions with experimental results [7] and as a possible method for extracting information on the magnitude of the axial-vector coupling constant g_A [8–10]. The Q value also defines the endpoint of the β-decay energy spectrum, which provides a strong test of systematics for detectors used to observe these decays, e.g., as was done in the case of ^{113}Cd [11]. In addition we report improved values for the atomic masses of ^{46,47,49,50}Ti, ^{50,51}V, and $^{50,52-54}$Cr. These results are important for testing the reliability of input data used in global evaluations of atomic masses, i.e., the atomic mass evaluation [12], and improving its overall accuracy.

II. EXPERIMENTAL METHOD

The Low Energy Beam and Ion Trap (LEBIT) facility located at the National Superconducting Cyclotron Laboratory (NSCL) was used to perform Q-value and absolute atomic mass determinations by measuring the cyclotron frequencies of singly charged titanium, vanadium, and chromium ions in a Penning trap. The LEBIT facility was designed for online mass measurements of rare isotopes produced at the NSCL [13]. However, offline sources, including a plasma source and

*redsh1m@cmich.edu
†Present address: Department of Physics, University of Notre Dame, Notre Dame, Indiana, 46556, USA.

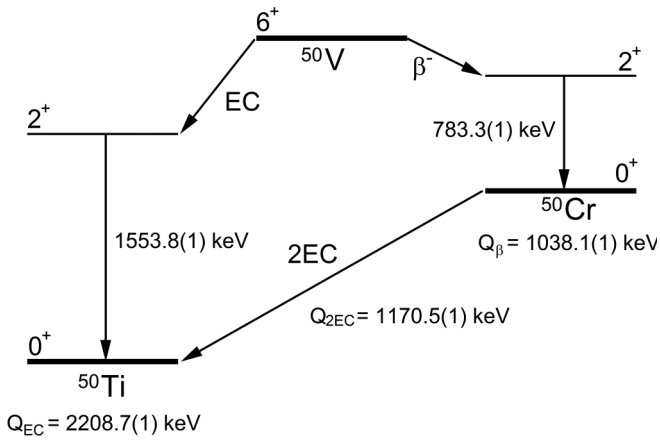

FIG. 1. Nuclear level scheme for β decay and electron-capture decay of ^{50}V and double electron capture decay of ^{50}Cr. The Q values are the ground-state to ground-state transition Q values, i.e., the energy equivalent of the mass difference between parent and daughter atoms.

a recently commissioned laser ablation source (LAS) [14], enable access to a wide range of stable and long-lived isotopes. Ions from these sources are used for calibration purposes and for mass and Q-value determinations with applications, for example, in nuclear and neutrino physics [11,15–20]. A schematic diagram of the sections of the LEBIT facility used in this work is shown in Fig. 2.

The LAS employs a frequency doubled pulsed Nd:YAG laser that can deliver up to 160 mJ per 4 ns pulse. The laser beam is focused onto an ablation target with a sub-mm spot size to produce power densities of up to $\sim 10^8$ W/cm^2. In this measurement campaign, high-purity titanium, vanadium, and chromium foils, typically 0.5–1 mm thick, with natural isotopic abundances were installed in the LAS. As such, ions of all naturally occurring isotopes of these elements could be produced: $^{46–50}$Ti, ^{50,51}V, $^{50,52–54}$Cr. Of these isotopes, ^{50}V has the lowest natural abundance (0.25%). Nevertheless, it was possible to produce sufficient quantities of ^{50}V$^+$ ions and remove ^{51}V$^+$ and any other contaminants from the beam and trap, as described below.

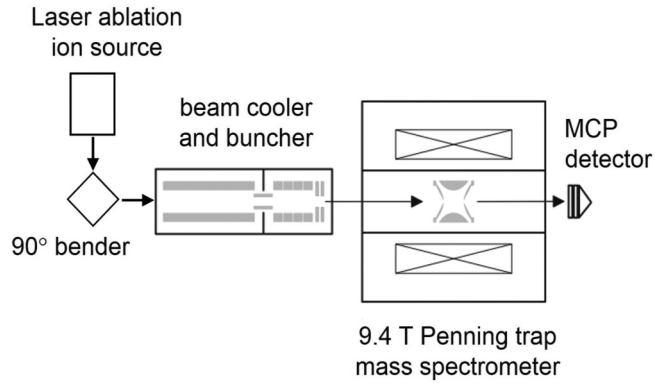

FIG. 2. Schematic diagram showing the subset of components of the LEBIT facility used in this work.

After the laser pulse is incident on the target material, ablated ions are extracted from the surface of the target and accelerated to 5 keV. Ions are then bent through 90° by a quadrupole bender and directed into a beam cooler and buncher [21,22]. In the cooler-buncher ions are thermalized via their interaction with a low-pressure helium buffer gas inside a linear radio frequency (rf) quadrupole trap. Thermalized ions are accumulated in an axial potential well superimposed over the rf trapping field before being ejected as a low-emittance, $\sim$100 ns duration ion bunch. Ions are then accelerated to 2 keV and transported toward the Penning trap. Before entering the fringe field of the magnet the ions pass through a fast-switching electrostatic gate which allows ions of a single A/q to pass through while all other ions in the beam are rejected. After they enter the magnetic field, ions are decelerated by a series of retarding electrodes before being captured in the Penning trap. The final retardation electrode is radially four-way segmented to create a "Lorentz" steerer, enabling precise control over the ion's initial radial amplitude and phase in the Penning trap [23].

The LEBIT Penning trap consists of an eightfold segmented hyperbolic ring electrode, two hyperbolic endcap electrodes, and two correction ring and correction tube electrodes [24], and is housed inside a 9.4 T superconducting solenoidal magnet. The electrodes produce a quadratic electrostatic potential that confines the ions axially along the direction of the magnetic field. Radial confinement is provided by the magnetic field that, in the absence of an electric field, causes the ions to undergo cyclotron motion at the free-space cyclotron frequency

$$f_c = \frac{1}{2\pi}\frac{qB}{m}. \tag{1}$$

The addition of the electric field results in three normal modes of motion for an ion in the Penning trap: the trap-cyclotron, magnetron, and axial modes, with frequencies f_+, f_-, and f_z, respectively. The free-space cyclotron frequency and the radial normal-mode frequencies are related via [25,26]

$$f_c = f_+ + f_-. \tag{2}$$

For more details on Penning trap physics see, for example, the review articles of Refs. [27,28].

After ions are captured in the Penning trap, contaminant ions are removed from the trap by applying a pulsed rf dipole drive at their trap-cyclotron frequency. The time-of-flight ion cyclotron resonance (TOF-ICR) technique [29] is then used to measure the cyclotron frequency of the ion of interest. This technique is well documented in the literature so is only briefly reviewed here.

A quadrupole rf drive at the frequency $f_{\rm rf}$ close to the sum frequency $f_+ + f_-$ is applied to ions in the Penning trap, which couples their magnetron and cyclotron modes. The drive amplitude and duration are chosen such that, when the correct frequency is applied, a full conversion is made of the ions' initial magnetron motion into cyclotron motion. Next the ions are ejected from the trap toward a microchannel plate detector (MCP) located in the fringe field of the magnet. Due to the interaction of the ions' magnetic moment with the magnetic-field gradient, the time of flight to the MCP depends on the ions' cyclotron amplitude in the trap. Thus, when

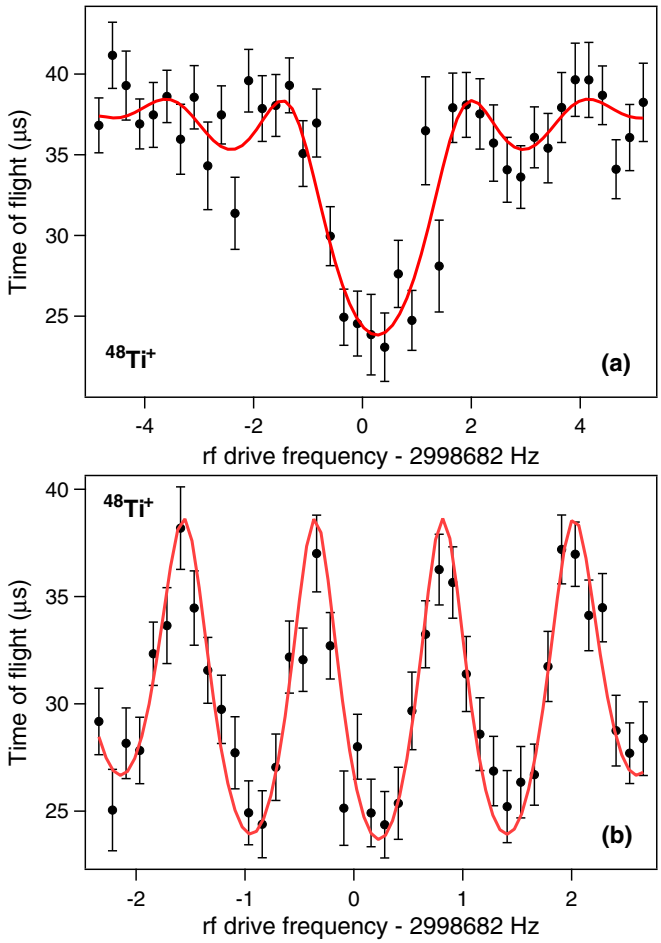

FIG. 3. Time-of-flight ion cyclotron frequency resonances for $^{48}Ti^+$ using (a) a 0.5 s traditional quadrupole excitation scheme, and (b) a 1.0 s Ramsey quadrupole excitation scheme. The solid lines are fits of the theoretical lineshapes to the data for the traditional [30] or Ramsey [33] schemes.

$f_{rf} = f_+ + f_-$, the cyclotron amplitude is maximized and the time of flight is minimized. To determine the optimal value of f_{rf} that minimizes the time of flight, a series of measurements are performed on sequentially trapped ion bunches in which f_{rf} is systematically varied, and a TOF resonance curve such as the one shown in Fig. 3(a) is obtained. A fit of the theoretical lineshape [30] to this curve is then used to extract the value of f_{rf} for the minimum time of flight that, according to Eq. (2), corresponds to the free-space cyclotron frequency.

For the data used in our final analysis, a Ramsey quadrupole excitation scheme was used to couple the magnetron and cyclotron modes [31,32]. This scheme modifies the TOF curve to that of Fig. 3(b), which is again fit with the theoretical lineshape [33]. This technique results in a narrower central peak in the TOF curve compared with the traditional TOF-ICR technique, and a factor of $\sim$3 increase in precision in f_c for the same measurement time.

To calibrate the magnetic field and to account for its time variation, cyclotron frequency measurements on the ion of interest, f_c^{ion}, and a reference ion, f_c^{ref}, are alternately performed. Typically, two reference ion measurements at

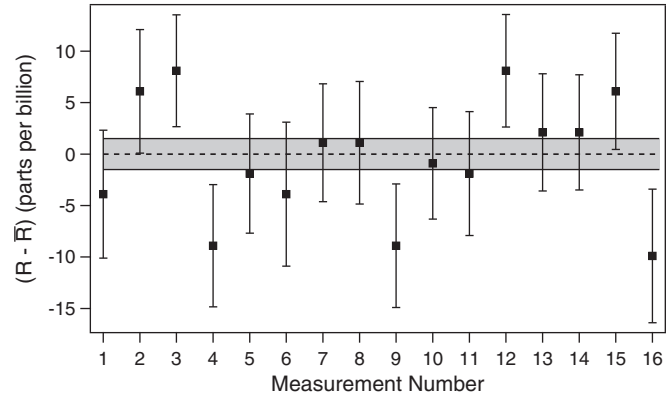

FIG. 4. Individual cyclotron frequency ratio measurements, R, of $^{50}V^+/^{50}Cr^+$, each obtained from pairs of frequency measurements similar to that of Fig. 3(b) and calculated by using Eq. (3). The dotted line and shaded region indicate the weighted average and corresponding uncertainty, as listed in Table I.

times t_0 and t_2 encompass each measurement of the ion of interest at time t_1. The frequencies of the reference ion measurements are interpolated to obtain f_c^{ref} at time t_1. The cyclotron frequency ratio, which corresponds to the inverse mass ratio of the ions, is thus obtained:

$$R = \frac{f_c^{ref}(t_1)}{f_c^{ion}(t_1)} = \frac{m_{ion} - m_e + b_{ion}/c^2}{m_{ref} - m_e + b_{ref}/c^2}. \quad (3)$$

Here, m_{ref} and m_{ion} are the neutral atomic masses of the reference and nuclide of interest, respectively, b_{ref} and b_{ion} are (in this case for singly charged atoms) their first ionization energies, m_e is the mass of the electron, and c is the speed of light. The cyclotron frequency ratio is obtained for all such alternating pairs of cyclotron frequency measurements and the average ratio $\bar{R}$ for the data set is obtained as a weighted average.

III. DATA AND ANALYSIS

In this work a 200-600-200 ms rf on-off-on two-pulse Ramsey scheme was used. A frequency range of $\pm$2.5 Hz around the resonant frequency was scanned in 125 mHz steps and typically 1 to 2 ions were detected per shot, producing a Ramsey TOF resonance, such as that shown in Fig. 3(b). When the number of detected ions was greater than five, these data were removed from the analysis to eliminate possible systematic frequency shifts due to the Coulomb interaction between ions in the trap [34–36]. The scan over the entire frequency range was repeated 30 times to accumulate statistics. As such, each resonance took about 30 mins to acquire and typically contained around 2000 detected ions.

For each ion pair for which the cyclotron frequency ratio was measured, between 9 and 33 individual ratio measurements were obtained by using Eq. (3) and the average ratio was found. Figure 4 shows an example of cyclotron frequency ratio data for $^{50}V^+/^{50}Cr^+$. For each of these data sets, the Birge ratio [37] was calculated. In cases where the Birge ratio BR was greater than 1, the statistical uncertainty in $\bar{R}$ was inflated by the factor BR. The resulting ratios are listed in Table I.

TABLE I. Average cyclotron frequency ratios $\bar{R}$ for the ion pairs listed with statistical uncertainties in parentheses. N is the number of measurements used to determine the average for each ion pair, and BR is the Birge ratio.

Num.	Ion pair	N	BR	$\bar{R}$
(1)	$^{50}V^+/^{50}Ti^+$	11	0.79	0.9999525266(23)
(2)	$^{50}V^+/^{50}Cr^+$	16	0.98	0.9999776879(15)
(3)	$^{48}Ti^+/^{46}Ti^+$	21	0.95	0.9583853416(13)
(4)	$^{48}Ti^+/^{47}Ti^+$	21	0.97	0.9792234132(12)
(5)	$^{48}Ti^+/^{49}Ti^+$	21	0.83	1.0208546008(11)
(6)	$^{48}Ti^+/^{50}Ti^+$	33	0.85	1.0416465817(10)
(7)	$^{48}Ti^+/^{50}V^+$	12	0.87	1.0416960347(23)
(8)	$^{48}Ti^+/^{51}V^+$	16	1.08	1.0624855042(17)
(9)	$^{48}Ti^+/^{50}Cr^+$	11	0.75	1.0416727876(15)
(10)	$^{48}Ti^+/^{52}Cr^+$	10	1.03	1.0832696834(20)
(11)	$^{48}Ti^+/^{53}Cr^+$	9	0.97	1.1041288205(24)
(12)	$^{48}Ti^+/^{54}Cr^+$	9	1.37	1.1249481224(33)

The main goal of this work was to measure the ^{50}V Q_{EC} and Q_β values, and the ^{50}Cr Q_{2EC} value. These quantities are defined as the energy equivalent of the mass difference between relevant parent and daughter atoms,

$$Q = [m_p - m_d]c^2, \tag{4}$$

where m_p and m_d are the mass of the parent and daughter atoms, respectively. Atomic masses can be obtained from Eq. (3), which can be arranged in the form of a mass difference equation,

$$m_{ref} - m_{ion} = [m_{ref} - m_e](1 - \bar{R}) + \frac{b_{ion}}{c^2} - \frac{b_{ref}}{c^2}\bar{R}. \tag{5}$$

Thus, the Q value can be indirectly determined from two ratio measurements that are used to determine the atomic masses of parent and daughter atoms, respectively. Alternatively, if the reference ion and ion of interest are chosen to be ions of the parent and daughter atoms, respectively, the Q value can be obtained directly from a single ratio measurement:

$$Q = [(m_p - m_e)c^2 + b_p](1 - \bar{R}) + b_d - b_p, \tag{6}$$

where the subscripts "p" and "d" refer to the parent and daughter atoms, respectively. In this work, singly charged titanium, chromium, and vanadium ions were used. The corresponding first ionization energies are $b_{Ti} = 6.83$ eV, $b_{Cr} = 6.77$ eV, $b_V = 6.75$ eV [38]. We note that the uncertainties in these ionization energies (all <10 meV), and any differences among the different isotopes of each element are insignificant at the level of precision of this work.

IV. RESULTS AND DISCUSSION

A. Q values among ^{50}Ti, ^{50}V, and ^{50}Cr

The ^{50}V Q_{EC} and Q_β values were obtained with Eq. (6) using the ratios (1) and (2) listed in Table I. The mass of the parent atom, in this case ^{50}V, does appear on the right-hand side of Eq. (6). For this calculation we used the new value for $m(^{50}V)$ obtained in this work—see Sec. IV B—and the conversion factor 931 494.0954(57) keV/c^2 per u [39] to obtain the Q value in keV. However, we note that the sensitivity of the calculated Q value to the uncertainty in the mass of the parent atom is reduced by a factor $(1 - \bar{R}) < 10^{-4}$, which is completely negligible at our level of precision. We also obtained the $^{50}V \rightarrow {}^{50}Cr$ β-decay Q value indirectly from Eq. (4) by using ratios (7) and (9) and Eq. (5) to determine the mass of ^{50}V and ^{50}Cr, respectively. Ratios (7) and (9) use the same reference ion $^{48}Ti^+$, so the uncertainty in the reference ion mass drops out in the Q-value determination. The Q value obtained from these two independent determinations agreed at the 1.5σ level. To account for the possible discrepancy between the two measurements we followed the procedure of the Particle Data Group [40] and inflated the uncertainty in the average by the factor 1.5, which corresponds to the scale factor defined in Ref. [40].

TABLE II. Q values (in keV) for the β decay and EC decay of ^{50}V and the 2EC decay of ^{50}Cr obtained from the cyclotron frequency ratios listed in Table I.

Decay	Ref.	Q value (keV)		ΔQ
		This work	AME2016	(keV/c^2)
^{50}V(EC)	Direct	2208.70(11)	2207.65(43)	1.05(44)
^{50}V(β^-)	Direct	1038.07(7)		
	^{48}Ti	1038.28(12)		
	Avg.	1038.12(9)	1038.06(59)	0.06(60)
^{50}Cr(2EC)	^{50}V	1170.63(13)		
	^{48}Ti	1170.43(8)		
	Avg.	1170.48(10)	1169.59(45)	0.90(46)

Finally, we obtained the ^{50}Cr Q_{2EC} value indirectly in two ways—by determining the ^{50}Cr and ^{50}Ti masses from ratios (1) and (2) using ^{50}V as a reference, and by determining the ^{50}Cr and ^{50}Ti masses from ratios (6) and (9) using ^{48}Ti as a reference (again, the uncertainty due to the reference ions then drops out). Here, the Q value obtained from the two methods agreed at the 1.4σ level and so we inflated the uncertainty in the average by 1.4.

The resulting Q values obtained from the different methods, the average values, and a comparison with values from the 2016 Atomic Mass Evaluation (AME2016) [12] are listed in Table II. We find that our result for the ^{50}V Q_β value is in good agreement with the AME2016 data, whereas our ^{50}V Q_{EC} and ^{50}Cr Q_{2EC} measurements show a 2σ shift of around 1 keV compared with the AME2016. As discussed in Sec. IV B, this shift is due to the fact that our values for the atomic masses of ^{50}V and ^{50}Cr are shifted from the AME2016 values by about 1 keV.

B. Atomic mass determinations for ^{46,47,49,50}Ti, ^{50,51}V, and $^{50,52-54}$Cr

The absolute masses of ^{46,47,49,50}Ti, ^{50,51}V, and $^{50,52-54}$Cr were determined from the cyclotron frequency ratio measurements (3)–(12) in Table I and by using Eq. (5). In each case $^{48}Ti^+$ was the reference ion and the value $m(^{48}Ti) =$ 47.947 940 932(117) u given in the AME2016 [12] was used.

TABLE III. Mass excesses (ME) for ^{46,47,49,50}Ti, ^{50,51}V, and $^{50,52-54}$Cr obtained from the cyclotron frequency ratios listed in Table I and mass differences ΔM between the AME2016 [12] values and our new results. The uncertainties given in parentheses in the second column correspond to the statistical uncertainty, uncertainty in the reference (^{48}Ti), and total uncertainty, respectively.

Isotope	ME (keV/c^2)		ΔM
	This work	AME2016	(keV/c^2)
^{46}Ti	−44128.06(6)(11)(12)	−44127.80(16)	0.26(21)
^{47}Ti	−44937.35(5)(11)(12)	−44937.37(11)	−0.02(17)
^{49}Ti	−48563.76(5)(11)(12)	−48563.79(11)	−0.03(17)
^{50}Ti	−51431.58(4)(11)(12)	−51431.66(12)	−0.08(17)
^{50}V	−49222.88(10)(11)(15)	−49224.02(41)	−1.14(43)
^{51}V	−52202.87(8)(11)(13)	−52203.85(40)	−0.98(42)
^{50}Cr	−50261.16(7)(11)(13)	−50262.08(44)	−0.92(45)
^{52}Cr	−55419.13(9)(11)(14)	−55419.25(34)	−0.11(37)
^{53}Cr	−55287.58(11)(11)(15)	−55287.01(35)	0.57(38)
^{54}Cr	−56935.17(15)(11)(18)	−56934.77(35)	0.40(40)

This value is mainly determined from precise Penning trap measurements of the atomic mass of ^{48}Ca [15] and of the ^{48}Ca–^{48}Ti double β-decay Q value [16,41]. A recent Penning trap determination of the mass of ^{48}Ca [42], not included in AME2016, reduces its uncertainty by a factor of ∼10 but is in agreement with the result of Ref. [15].

Our resulting atomic masses were converted into mass excesses and are listed in Table III. The difference between our results and the AME2016 values are also listed in Table III and are plotted in Fig. 5.

1. Atomic masses of ^{46,47,49,50}Ti

Our results for the atomic masses of ^{47,49,50}Ti are in excellent agreement with the values listed in the AME2016. These values are either completely or mainly determined from (n,γ) reactions, i.e., neutron binding energy measurements, performed via γ-ray spectroscopy after neutron capture on ^{47,48,49}Ti, which link them to the mass of ^{48}Ti. Our value for the mass of ^{46}Ti is also in good agreement with the AME2016 value, which was determined via (p,γ), $(^3\text{He},t)$, and (d,p) reactions. Due to the uncertainty in the mass of ^{48}Ti of 0.11 keV, our new results do not reduce the uncertainties in the masses of ^{47,49,50}Ti, but reduce the ^{46}Ti uncertainty by a factor of 1.3 compared with the AME2016.

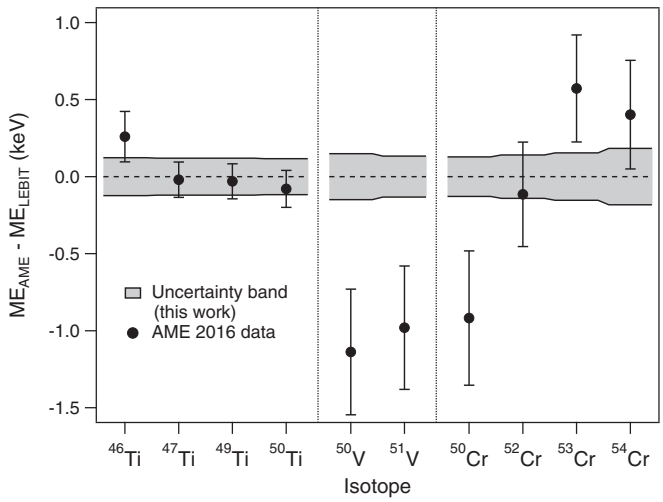

FIG. 5. Difference between mass excesses given in the AME2016 and those determined in this work. The shaded band corresponds to the total uncertainty in our mass measurements, as listed in the second column of Table III.

TABLE IV. Neutron separation energies obtained via cyclotron frequency ratio measurements described here, E_n, and from γ-ray spectroscopy measurements performed after neutron capture on ^{47,48,49}Ti, E_γ [43,44].

Isotope	E_n (keV)	E_γ (keV)	$E_\gamma - E_n$ (keV)
^{48}Ti	11626.68(5)	11626.65(4)	−0.03(7)
^{49}Ti	8142.37(5)	8142.39(3)	0.02(6)
^{50}Ti	10939.14(7)	10939.19(3)	0.05(7)

2. Neutron separation energies of ^{48,49,50}Ti

From our cyclotron frequency ratio measurements of ^{48}Ti$^+$/^{47}Ti$^+$, ^{48}Ti$^+$/^{49}Ti$^+$, and ^{48}Ti$^+$/^{50}Ti$^+$, and by using Eq. (5), we can obtain the mass difference Δm between ^{47}Ti-^{48}Ti, ^{48}Ti-^{49}Ti, and ^{49}Ti-^{50}Ti. Hence, we can determine the neutron separation energy $E_n = m_n - \Delta m$, where m_n is the mass of the neutron. These results can be directly compared with the (n,γ) measurements of Refs. [43,44] that are used in the AME2016 evaluation; see Table IV. This comparison provides a test of $E = mc^2$, similar to that described in Ref. [45], but is a factor of about 10 less precise. However, improvements in the precision of the mass measurements are possible with existing or upcoming facilities; see, e.g., Refs. [46,47], and the γ-ray spectroscopy measurement could be performed more precisely by using the GAMS4 crystal diffraction spectrometer [48].

3. Atomic masses of ^{50,51}V

Our new results for the mass of ^{50,51}V indicate a shift of about 1 keV with respect to the AME2016 and an increase in precision of a factor of three in both cases. The mass of ^{50}V is determined from nuclear reaction data, whereas the mass of ^{51}V was determined from a Penning trap measurement [49] and from (p,n) reaction data, linking it to ^{51}Cr [50]. The ^{51}Cr mass was also determined in the Penning trap measurement of Ref. [49]. Our value for $m(^{51}\text{V})$ and that of Ref. [49] differ by 0.82(55) keV, i.e., 1.5σ.

4. Atomic masses of $^{50,52-54}$Cr

For the chromium masses, our results indicate that the AME2016 value for ^{50}Cr is too low by about 1 keV; a 2σ difference. The value for ^{54}Cr is too large by 0.6 keV (1.5σ) and the values for ^{52,53}Cr agree at the 1σ level or better. In each case we improve the uncertainties by factors of ∼2–3. Only ^{52}Cr was previously determined via a direct

Penning trap measurement. This measurement was performed with the ISOLTRAP facility and was included in AME2016, but is currently unpublished [51]. Neutron capture (n,γ) measurements link the ^{53,54}Cr masses to ^{52}Cr and the ^{50}Cr mass to ^{51}Cr.

V. CONCLUSION

We have performed the first direct measurement of the ^{50}V β decay and electron-capture Q values and have also provided a new determination of the ^{50}Cr double electron-capture Q value by using high-precision Penning trap mass spectrometry. These results provide precise input data for theoretical calculations of these processes and can be used to help analyze experimental data. We also report on the first measurements of the masses of ^{46,47,49,50}Ti, ^{50}V, and ^{50,53,54}Cr via Penning trap mass spectrometry, and provide more precise mass values for ^{51}V, and ^{52}Cr, which have been previously measured with Penning traps.

ACKNOWLEDGMENTS

This research was supported by Michigan State University and the Facility for Rare Isotope Beams, the National Science Foundation under Contracts No. PHY-1102511 and No. PHY-1307233, and the Central Michigan University Faculty Research and Creative Endeavors grant program. This material is based upon work supported by the US Department of Energy, Office of Science, Office of Nuclear Physics under Award No. DE-SC0015927. The work leading to this publication has also been supported by a DAAD P.R.I.M.E. fellowship with funding from the German Federal Ministry of Education and Research and the People Programme (Marie Curie Actions) of the European Union's Seventh Framework Programme (FP7/2007/2013) under REA Grant Agreement No. 605728.

[1] H. Dombrowski, S. Neumaier, and K. Zuber, Phys. Rev. C **83**, 054322 (2011).
[2] I. Bikit, N. Zikić-Todorović, J. Slivka, M. Vesković, M. Krmar, L. Čonkić, J. Puzović, and I. V. Aničin, Phys. Rev. C **67**, 065801 (2003).
[3] D. E. Alburger, E. K. Warburton, and J. B. Cumming, Phys. Rev. C **29**, 2294 (1984).
[4] J. J. Simpson, P. Jagam, and A. A. Pilt, Phys. Rev. C **31**, 575 (1985).
[5] J. J. Simpson, P. Moorhouse, and P. Jagam, Phys. Rev. C **39**, 2367 (1989).
[6] M. Haaranen, P. C. Srivastava, J. Suhonen, and K. Zuber, Phys. Rev. C **90**, 044314 (2014).
[7] F. Quarati, P. Dorenbos, and X. Mougeot, Appl. Radiat. Isot. **108**, 30 (2016).
[8] M. Haaranen, P. C. Srivastava, and J. Suhonen, Phys. Rev. C **93**, 034308 (2016).
[9] M. Haaranen, J. Kotila, and J. Suhonen, Phys. Rev. C **95**, 024327 (2017).
[10] J. Kostensalo, M. Haaranen, and J. Suhonen, Phys. Rev. C **95**, 044313 (2017).
[11] N. D. Gamage, G. Bollen, M. Eibach, K. Gulyuz, C. Izzo, R. M. E. B. Kandegedara, M. Redshaw, R. Ringle, R. Sandler, and A. A. Valverde, Phys. Rev. C **94**, 025505 (2016).
[12] M. Wang, G. Audi, F. Kondev, W. Huang, S. Naimi, and X. Xu, Chin. Phys. C **41**, 030003 (2017).
[13] R. Ringle, G. Bollen, and S. Schwarz, Int. J. Mass Spectrom. **349–350**, 87 (2013).
[14] C. Izzo, G. Bollen, S. Bustabad, M. Eibach, K. Gulyuz, D. J. Morrissey, M. Redshaw, R. Ringle, R. Sandler, S. Schwarz, and A. A. Valverde, Nucl. Instrum. Methods Phys. Res., Sect. B **376**, 60 (2015).
[15] M. Redshaw, G. Bollen, M. Brodeur, S. Bustabad, D. L. Lincoln, S. J. Novario, R. Ringle, and S. Schwarz, Phys. Rev. C **86**, 041306 (2012).
[16] S. Bustabad, G. Bollen, M. Brodeur, D. L. Lincoln, S. J. Novario, M. Redshaw, R. Ringle, S. Schwarz, and A. A. Valverde, Phys. Rev. C **88**, 022501 (2013).
[17] S. Bustabad, G. Bollen, M. Brodeur, D. L. Lincoln, S. J. Novario, M. Redshaw, R. Ringle, and S. Schwarz, Phys. Rev. C **88**, 035502 (2013).
[18] D. L. Lincoln, J. D. Holt, G. Bollen, M. Brodeur, S. Bustabad, J. Engel, S. J. Novario, M. Redshaw, R. Ringle, and S. Schwarz, Phys. Rev. Lett. **110**, 012501 (2013).
[19] K. Gulyuz, J. Ariche, G. Bollen, S. Bustabad, M. Eibach, C. Izzo, S. J. Novario, M. Redshaw, R. Ringle, R. Sandler, S. Schwarz, and A. A. Valverde, Phys. Rev. C **91**, 055501 (2015).
[20] M. Eibach, G. Bollen, K. Gulyuz, C. Izzo, M. Redshaw, R. Ringle, R. Sandler, and A. A. Valverde, Phys. Rev. C **94**, 015502 (2016).
[21] S. Schwarz, G. Bollen, D. Lawton, A. Neudert, R. Ringle, P. Schury, and T. Sun, Nucl. Instrum. Methods Phys. Res., Sect. B **204**, 474 (2003).
[22] S. Schwarz, G. Bollen, R. Ringle, J. Savory, and P. Schury, Nucl. Instrum. Methods Phys. Res., Sect. A **816**, 131 (2016).
[23] R. Ringle, G. Bollen, A. Prinke, J. Savory, P. Schury, S. Schwarz, and T. Sun, Int. J. Mass Spectrom. **263**, 38 (2007).
[24] R. Ringle, G. Bollen, A. Prinke, J. Savory, P. Schury, S. Schwarz, and T. Sun, Nucl. Instrum. Methods Phys. Res., Sect. A **604**, 536 (2009).
[25] G. Gabrielse, Phys. Rev. Lett. **102**, 172501 (2009).
[26] G. Gabrielse, Int. J. Mass Spectrom. **279**, 107 (2009).
[27] L. S. Brown and G. Gabrielse, Rev. Mod. Phys. **58**, 233 (1986).
[28] K. Blaum, Phys. Rep. **425**, 1 (2006).
[29] G. Gräff, H. Kalinowsky, and J. Traut, Z. Phys. A: At. Nucl. **297**, 35 (1980).
[30] M. König, G. Bollen, H.-J. Kluge, T. Otto, and J. Szerpo, Int. J. Mass Spectrom. Ion Processes **142**, 95 (1995).
[31] G. Bollen, H.-J. Kluge, T. Otto, G. Savard, and H. Stolzenberg, Nucl. Instrum. Methods Phys. Res., Sect. B **70**, 490 (1992).
[32] S. George, K. Blaum, F. Herfurth, A. Herlert, M. Kretzschmar, S. Nagy, S. Schwarz, L. Schweikhard, and C. Yazidjian, Int. J. Mass Spectrom. **264**, 110 (2007).
[33] M. Kretzschmar, Int. J. Mass Spectrom. **264**, 122 (2007).
[34] R. S. Van Dyck, F. L. Moore, D. L. Farnham, and P. B. Schwinberg, Phys. Rev. A **40**, 6308 (1989).

[35] G. Bollen, H.-J. Kluge, M. König, T. Otto, G. Savard, H. Stolzenberg, R. B. Moore, G. Rouleau, G. Audi, and ISOLDE Collaboration, Phys. Rev. C **46**, R2140(R) (1992).
[36] A. Kellerbauer, K. Blaum, G. Bollen, F. Herfurth, H.-J. Kluge, M. Kuckein, E. Sauvan, C. Scheidenberger, and L. Schweikhard, Eur. Phys. J. D **22**, 53 (2003).
[37] R. T. Birge, Phys. Rev. **40**, 207 (1932).
[38] *NIST Chemistry WebBook*, NIST Standard Reference Database Number 69, edited by P. J. Linstrom and W. G. Mallard (National Institute of Standards and Technology, Gaithersburg, 2016); http://webbook.nist.gov (retrieved May 24, 2016).
[39] P. J. Mohr, D. B. Newell, and B. N. Taylor, Rev. Mod. Phys. **88**, 035009 (2016).
[40] C. Patrignani and P. D. Group, Chin. Phys. C **40**, 100001 (2016).
[41] A. A. Kwiatkowski, T. Brunner, J. D. Holt, A. Chaudhuri, U. Chowdhury, M. Eibach, J. Engel, A. T. Gallant, A. Grossheim, M. Horoi, A. Lennarz, T. D. Macdonald, M. R. Pearson, B. E. Schultz, M. C. Simon, R. A. Senkov, V. V. Simon, K. Zuber, and J. Dilling, Phys. Rev. C **89**, 045502 (2014).
[42] F. Köhler, K. Blaum, M. Block, S. Chenmarev, S. Eliseev, D. Glazov, M. Goncharov, J. Hou, A. Kracke, D. Nesterenko, Y. N. Novikov, W. Quint, E. M. Ramirez, V. M. Shabaev, A. Volotka, and G. Werth, Nat. Commun. **7**, 10246 (2016).
[43] J. Ruyl and P. Endt, Nucl. Phys. A **407**, 60 (1983).
[44] J. Ruyl, J. D. Haas, P. Endt, and L. Zybert, Nucl. Phys. A **419**, 439 (1984).
[45] S. Rainville, J. K. Thompson, E. G. Myers, J. M. Brown, M. S. Dewey, E. G. Kessler, Jr., R. D. Deslattes, H. G. Börner, M. Jentschel, P. Mutti, and D. E. Pritchard, Nature (London) **438**, 1096 (2005).
[46] M. Redshaw, J. McDaniel, and E. G. Myers, Phys. Rev. Lett. **100**, 093002 (2008).
[47] M. Redshaw, R. Bryce, P. Hawks, N. Gamage, C. Hunt, R. Kandegedara, I. Ratnayake, and L. Sharp, Nucl. Instrum. Methods Phys. Res., Sect. B **376**, 302 (2016).
[48] M. S. Dewey and E. G. Kessler, Jr., J. Res. Natl. Inst. Stand. Technol. **105**, 11 (2000).
[49] T. D. Macdonald, B. E. Schultz, J. C. Bale, A. Chaudhuri, U. Chowdhury, D. Frekers, A. T. Gallant, A. Grossheim, A. A. Kwiatkowski, A. Lennarz, M. C. Simon, V. V. Simon, and J. Dilling, Phys. Rev. C **89**, 044318 (2014).
[50] H. Schölermann and R. Böttger, Nucl. Phys. A **501**, 86 (1989).
[51] M. Mougeot, for the ISOLTRAP Collaboration (private communication).